Chemical Engineering Journal 303 (2016) 1–13

Contents lists available at ScienceDirect

Chemical Engineering Journal

journal homepage: www.elsevier.com/locate/cej

A novel approach for methylene blue removal by calcium dodecyl sulfate enhanced precipitation and microbial flocculant GA1 flocculation

Zhaohui Yang *, Min Li, Mingda Yu, Jing Huang, Haiyin Xu, Yan Zhou, Peipei Song, Rui Xu

College of Environmental Science and Engineering, Hunan University, Changsha 410082, PR China
Key Laboratory of Environmental Biology and Pollution Control (Hunan University), Ministry of Education, Changsha 410082, PR China

HIGHLIGHTS

- A novel approach for the efficient removal of MB was proposed.
- SDS solubilization and Ca^{2+} effect were combined to reduce the solubility of MB.
- MB precipitated from aqueous solution by adsorbing onto the Ca $(DS)_2$ particles.
- The $Ca(DS)_2$ particles adsorbed MB were flocculated by MBFGA1.

GRAPHICAL ABSTRACT

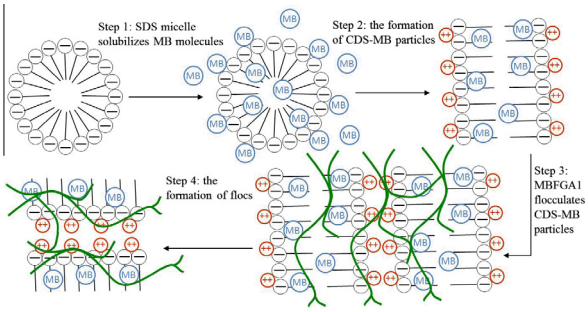

ARTICLE INFO

Article history:
Received 20 March 2016
Received in revised form 21 May 2016
Accepted 23 May 2016
Available online 26 May 2016

Keywords:
Methylene blue
Calcium dodecyl sulfate
Sodium dodecyl sulfate
Calcium ions
Microbial flocculant
Solubilization

ABSTRACT

A novel approach was proposed for the removal of methylene blue (MB), a soluble cationic dye, from aqueous solution by calcium dodecyl sulfate ($Ca(DS)_2$) enhanced precipitation which was based on the solubilization of sodium dodecyl sulfate (SDS) on MB and Ca^{2+} effect on SDS micelles, and microbial flocculant GA1 (MBFGA1) flocculation. The independent and interactive effects of factors, such as SDS, Ca^{2+} and MBFGA1 dosages, on the MB removal and interaction between SDS and Ca^{2+} were investigated. The response surface methodology (RSM), environmental scanning electron microscope (ESEM) and energy dispersive spectrometer (EDS) analysis were employed to discuss the interaction mechanism between SDS and Ca^{2+}, and MB removal mechanism. The results showed that MB and SDS removal efficiency could reach 98.63% and 88.97%, respectively, with pH (10), MB (50 mg/L), SDS (8 mM), Ca^{2+} (5 mM) and MBFGA1 (4 mL/L). Under the optimal conditions, residual SDS and Ca^{2+} concentrations in the upper phase were 0.88 mM and 1.27 mM, respectively, which reached the *K*sp of $Ca(DS)_2$. The concentration consumption ratio between SDS and Ca^{2+} was 2.0. The interaction between SDS and Ca^{2+} was depended on the SDS-Ca^{2+} concentration ratio in aqueous solution rather than the CMC of SDS. When Ca^{2+} concentration was relatively sufficient, SDS micelles containing the solubilized MB (SDS-MB micelles) would disassemble to generate MB loaded $Ca(DS)_2$ particles (CDS-MB particles) which would be flocculated by MBFGA1. Whereas, when SDS concentration was superfluous relatively, SDS micelles formed in the upper phase would redissolve the CDS-MB particles in flocs.

1. Introduction

Dyes and pigments are widely used in the textile and leather dyeing, printing, pharmaceutical, and cosmetic industries [1,2]. Discharge of the dyes to the environment have aroused serious

* Corresponding author at: College of Environmental Science and Engineering, Hunan University, Changsha 410082, PR China.
E-mail address: yzh@hnu.edu.cn (Z. Yang).

http://dx.doi.org/10.1016/j.cej.2016.05.101
1385-8947/

concerns all over the world due to the toxicity of dyeing effluents, such as carcinogenic and mutagenic action to aquatic biota and humans [1]. Furthermore, the dyes in surface water are aesthetically displeasing, imped sunlight penetration and reduce the dissolved oxygen, which cause annoyance to the aquatic biosphere [3]. Therefore, it is important to remove the dyes from wastewater to an acceptable level before discharging into the natural environment.

In recent years, several physical, chemical and biological methods, including adsorption [2,4,5], photo-catalytic degradation [6], biodegradation [7], micellar-enhanced ultrafiltration (MEUF) [1,8–10] and flocculation [11,12] have been developed to reduce the pollution and hazards of dyes. Among these methods, flocculation is considered as an attractive and favorable technique because its low capital cost, short detention time and good removal efficiency [3,13]. However, the main limitation of the conventional flocculation technique is that it cannot remove soluble dyes like methylene blue (MB) effectively as a main treatment [3]. Thus, it is crucial to reduce the solubility of MB, a soluble cationic dye, before employing flocculation technology.

Recently, sodium dodecyl sulfate (SDS), a widely used anionic surfactant, has been employed to improve the MB removal efficiency in the micellar enhanced ultrafiltration technique [1,9,10] and the surfactant enhanced adsorption technique [14,15], which owing to the micellar solubilization of SDS on MB molecules. That is when SDS concentration is equal to or higher than its critical micellar concentration (CMC), SDS monomers will assemble to form micelles which are capable of solubilizing MB molecules [1]. Furthermore, the interaction between SDS and calcium ion has been studied in many literatures [16–18]. These researches show that the interaction was depended on the CMC of SDS. Below its CMC of 8 mM, SDS monomers will react with calcium ions to generate precipitation, which is governed by the solubility product of calcium dodecyl sulfate (CDS), whereas, above the CMC, the precipitated CDS will be redissolved gradually by SDS micelles [16,18]. Though the solubilization of SDS and the interaction of SDS with calcium ion have both been researched widely, to our best knowledge, there is no research to combine those two chemical properties of SDS to reduce the solubility of MB.

In this study, the solubilization effect of SDS on MB and the calcium ion effect on SDS micelles containing the solubilized MB (SDS-MB micelles) were combined, for the first time, to make MB precipitate from aqueous solution in a form of suspended particles, which then were flocculated by microbial flocculant GA1 (MBFGA1). MBFGA1, a kind of microbial flocculant, is produced from *Paenibacillus polymyxa* GA1 with being eco-friendly, high security and high efficiency for removing Kaolin suspension which has been studied in our previous work [19–21]. The main objective of this research had two aspects: the one was to investigate the independent and interactive effects of factors, including SDS, calcium ions and MBFGA1 dosages, on the MB removal efficiency and the interaction between SDS and calcium ions, the other was to explore the interaction mechanism between SDS and Ca^{2+}, MB removal mechanism and flocculation mechanism based on the experimental results.

2. Materials and methods

2.1. Materials

The cationic dye, MB (DaMao Chemicals, China) was prepared by dilution of 1 g/L stock solution. Fresh diluents were used in each experiment. The anionic surfactant, SDS (Sinopharm Chemicals, China) was prepared at the concentration of 100 g/L. The critical micelle concentration (CMC) is 8 mM in distilled water [22]. $CaCl_2$ (Sanpu Chemicals, China) was prepared at the concentration of 10 g/L to provide Ca^{2+} which was crucial during the MB removal process. Microbial flocculant GA1 was harvested from the fermentation liquid of *Paenibacillus polymyxa* GA1 with high flocculation activity [19–21] and the fermentation liquid contained 15.56 g/L effective components. Unless otherwise stated, all reagents used were of analytically pure grade. The distilled water was used in all experiments.

2.2. MB removal experiment

1000 mL of MB solution was prepared at the concentration of 50 mg/L (Fig. S1). Then the pH of the MB solution was adjusted to 10 (Fig. S2) by NaOH and HCl, which was discussed specifically in the Supplementary Material. Subsequently, pre-determined amounts of SDS, $CaCl_2$ and MBFGA1 were added into the 1000 mL MB solution in 1000 mL beaker in turn. Then the beaker containing the mixture was fixed on the floc-tester (ET-720. Lovibond. Germany). After that, the mixture was stirred with 5 min rapid mixing at 200 rpm, followed by 30 min slow mixing at 40 rpm and 1 h settlement period. Water samples were collected at a depth of 2 cm in the upper phase for the zeta potential measurement and the concentration determination of MB, SDS and Ca^{2+}.

2.3. Analysis and calculations

The zeta potential and MB concentration were directly measured by Zetasizer (Nano-ZS90, Malvern, England) and UV spectrophotometer (UV-2550, SHIMADZU, Japan) at 665 nm, respectively. However, the water samples should be filtered through 0.45 μm filter membrane before the concentration measurements of SDS and Ca^{2+} were taken. The SDS concentration was analyzed by a double phase titration following ISO-2271-1989 using benzethonium chloride (J&K Chemicals, China) as standard and an indicator consisting in a mixture of ethidium bromide and acid blue 1 (Aladdin Industrial Corporation, China). The ethidium bromide was HPLC pure. Chloroform (Sinopharm Chemicals, China) was used to provide the double phase. The Ca^{2+} concentration was analyzed by EDTA (Sinopharm Chemicals, China) titrimetric method following ISO-6058-1984. All experiments were performed in triplicates for the mean calculation and the results were reproducible within 5%.

The removal efficiency (RE) of MB, SDS and Ca^{2+} all followed the equation:

$$\mathrm{RE}\,(\%) = (C_0 - C_e)/C_0 \times 100 \tag{1}$$

where C_0 denotes the initial concentration (dosage) of MB, SDS and Ca^{2+}; C_e denotes the final concentration in the upper phase of MB, SDS and Ca^{2+}.

We defined the concentration consumption of SDS or Ca^{2+} as:

$$\mathrm{Q} = C_1 - C_2 \tag{2}$$

where C_1 is the initial dosage of SDS or Ca^{2+} (mM); C_2 is the final concentration in the upper phase of SDS or Ca^{2+} (mM).

The concentration consumption ratio (CT) between SDS and Ca^{2+} was defined as:

$$\mathrm{CT} = Q_s/Q_c \tag{3}$$

where Q_S and Q_C are the concentration consumptions of SDS and Ca^{2+} (mM), respectively, which follows the Eq. (2).

Generally, at low SDS concentration, Ca^{2+} could react with SDS monomers as follows:

$$Ca^{2+} + DS^{-} \leftrightarrow Ca(DS)_2 \tag{4}$$

The solubility product *K*sp of $Ca(DS)_2$ at room temperature was calculated as [16]:

$$K_{sp} = [Ca^{2+}][DS^{-}]^2 = (8.2 \pm 1.9) \times 10^{-10}\ m^3 \quad (5)$$

2.4. RSM experimental design

The central composite design (CCD), a standard RSM, was selected for the optimization of the factors which made sense on the MB removal. In the experimental design model, the dosages of SDS (x_1), Ca^{2+} (x_2) and MBFGA1 (x_3) were taken as factors. All factors were controlled at five levels. The response variable (y) that represented the MB removal efficiency was fitted by a second-order model in the form of quadratic polynomial equation:

$$y = \beta_0 + \sum_{i=1}^{m}\beta_i x_i + \sum_{i<j}^{m}\beta_{ij} x_i x_j + \sum_{i=1}^{m}\beta_{ii} x_i^2 \quad (6)$$

where x_i and x_j are independent variables which determine y, β_0, β_i and β_{ii} are the offset term the i linear coefficient and the quadratic coefficient, respectively. β_{ij} is the term that reflects the interaction between x_i and x_j [23]. The actual design ran by the statistic software, Design-Expert 8.0.6 (Stat-Ease Inc., USA), is presented in Table 1.

2.5. Environmental scanning electron microscope (ESEM) analysis

When MB concentration, the dosages of Ca^{2+} and MBFGA1 were fixed at 50 mg/L, 5 mM and 4 mL/L, respectively, the corresponding flocs formed under different SDS concentrations of 8, 16, and 24 mM, were collected. After vacuum freeze-drying, the flocs were used for environmental scanning electron microscope analysis and energy dispersive spectrometer analysis.

The surface morphologies of samples were studied using an environmental scanning electron microscope (Quanta 200 FEG, FEI, USA) in low vacuum mode at an acceleration potential of 20 kV. Furthermore, microanalyses of the samples were carried out with an energy dispersive spectrometer (EDS) equipped on the Quanta 200.

3. Results and discussion

3.1. Effects of SDS dosage

3.1.1. Influence of SDS dosage on the MB removal

The MB concentration and MBFGA1 dosage were fixed at 50 mg/L and 4 mL/L, respectively. The variation of the MB removal efficiency with SDS dosage under different Ca^{2+} dosages was shown in Fig. 1(a). It was clear that when Ca^{2+} dosage was 5 mM, with SDS dosage increasing from 1.4 to 8 mM, the MB removal efficiency increased sharply from 50.08% to 98.63%, followed by decreasing linearly (approximately) to 30.08% with a SDS dosage of 12.6 mM, then decreased slowly to 0% at the SDS dosage of 48 mM.

From the figure, when the SDS dosage was lower than 8 mM, although it was usually considered that surfactant monomers did not form micelles, the MB removal efficiency was not low and increased quickly as SDS dosage increased. This phenomenon was attributed to the following three causes. The first reason was that the SDS molecules could form small premicelles below the CMC, which could result in the weak solubilization effect [10,24] and provide MB with a micellar-like environment [25]. However, when the SDS concentration exceeded one CMC value, the solubilization effect was in process obviously [26]. Secondly, MB could decrease the CMC of SDS slightly and make the formation of SDS micelles easier, probably because the MB molecules dissociated into cationic ions that could insert into the head groups of SDS leading to the reduction of electrostatic repulsive force between head groups of SDS micelles [1]. The third cause was the precipitation reaction of SDS with MB below the CMC [1,27].

Table 1
Coded levels for three variables framed by CCD.

Factors	Codes	Coded levels				
		−1.68	−1	0	1	1.68
SDS (mM)	x_1	1.27	4	8	12	14.73
Ca^{2+} (mM)	x_2	1.64	3	5	7	8.36
MBFGA1 (ml/L)	x_3	0.64	2	4	6	7.36

From Fig. 1(a), when Ca^{2+} dosage was 5 mM, the highest MB removal efficiency of 98.63% was achieved when SDS dosage was at its CMC of 8 mM. It was probably that at the CMC value, the SDS micelles had been formed absolutely which could solubilize the majority of MB molecules. Based on the former research results that Ca^{2+} could react with SDS monomers to generate CDS precipitation [16–18], we could speculate that in the system, the SDS micelles containing the solubilized MB kept dynamic equilibrium with the SDS monomers adsorbed MB (SDS-MB monomers) [17], the Ca^{2+} would gradually react with the SDS-MB monomers to generate MB loaded calcium dodecyl sulfate (CDS) particles (CDS-MB particles). The suspended CDS-MB particles would be flocculated by MBFGA1 finally. Therefore, it could be concluded that the 5 mM Ca^{2+} dosage was sufficient compared to the 8 mM SDS dosage, and the 8 mM SDS dosage was the point that the reaction between SDS-MB monomers and Ca^{2+} could proceed completely. Consequently, at 8 mM SDS dosage, the majority of MB molecules were removed in the form of CDS-MB particles.

When Ca^{2+} dosage was 5 mM, with the SDS dosage increasing from 8 to 12.6 mM, the MB removal efficiency decreased from 98.63% to 30.08% almost in a linear pattern, furthermore, the corresponding experimental phenomenon was that the amount of flocs in the beaker bottom gradually decreased and its color turned from blue to white. Therefore, we could speculate that when SDS dosage was higher than 8 mM, it was superfluous compared to the 5 mM Ca^{2+} dosage, and SDS micelles had been formed in the upper liquid phase. With the SDS dosage ranging from 8 to 12.6 mM, the most of MB adsorbed on the CDS particles would be solubilized by the SDS micelles in the upper liquid phase, which resulted in the resolubilization phenomenon of MB.

With continued increment of the SDS dosage from 12.6 to 48 mM, the MB removal efficiency decreased gradually to 0%, the white flocs kept reducing and disappeared at 48 mM SDS dosage. In addition, it was observed from Fig. 1(b) that when Ca^{2+} dosage was 5 mM, the Ca^{2+} concentration in the upper phase descended to the lowest value firstly, and then ascended. The minimum was obtained at 12.6 mM SDS dosage. Hence, based on the points stated above, it could be concluded that as SDS dosage increased from 12.6 to 48 mM, the SDS micelles in the upper liquid phase would adsorb the Ca^{2+} in CDS-MB particles leading to the dissolution of CDS-MB particles gradually [16,18]. As a result, the CDS-MB particles were dissolved completely and a clear blue solution appeared at 48 mM SDS dosage. The redissolution of Ca^{2+} would be discussed in detail in Section 3.1.2.

It could be seen from Fig. 1(a) that with the Ca^{2+} dosages being 7 mM and 9 mM, the variation trends of MB removal efficiencies were mostly similar to that at 5 mM Ca^{2+} dosage. That was as the SDS dosages increased from 1.4 to 80 mM, the MB removal efficiencies ascended to the maximum, and then decreased to 0%. When the Ca^{2+} dosages were 7 mM and 9 mM, the highest removal efficiencies of 98.82% and 99.10% were achieved at 12.6 mM and 16 mM SDS dosages, respectively. This phenomenon indicated that 7 mM and 9 mM Ca^{2+} dosages were sufficient compared to the 12.6 mM and 16 mM SDS dosages, hence, we could conclude that

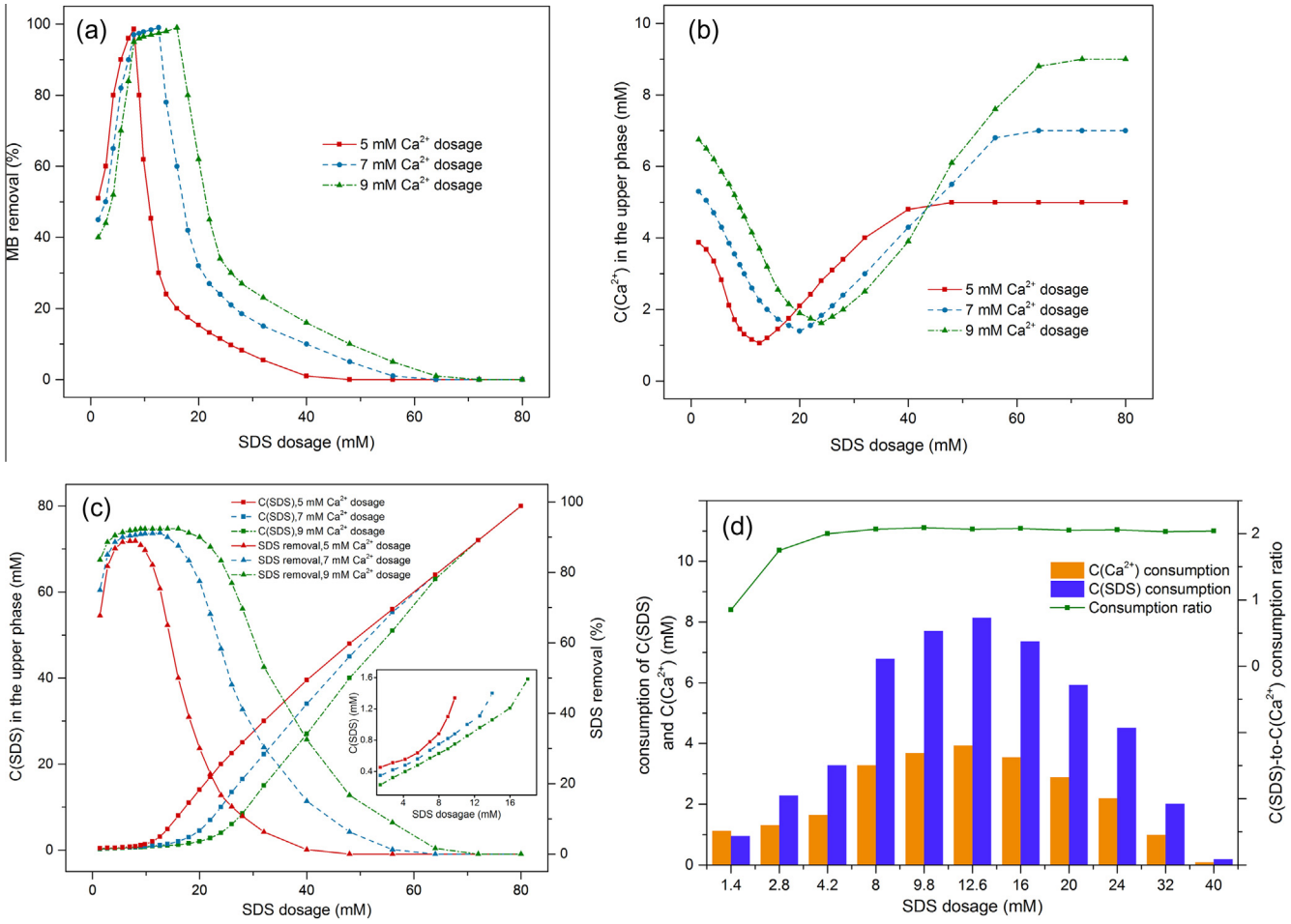

Fig. 1. Effects of SDS dosage on the (a) MB removal efficiency, (b) Ca^{2+} concentration in the upper phase, (c) SDS concentration in the upper phase and SDS removal efficiency at different Ca^{2+} dosages of 5, 7, and 9 mM; (d) SDS and Ca^{2+} concentration consumption and SDS-to-Ca^{2+} concentration consumption ratio at 5 mM Ca^{2+} dosage. The MB concentration and MBFGA1 dosage were 50 mg/L and 4 mL/L, respectively.

as long as Ca^{2+} concentration was sufficient relatively in the system, under the effect of Ca^{2+}, the SDS-MB micelles would disassemble gradually to generate CDS-MB particles even if the SDS concentration was above the CMC. This conclusion advanced the former research results [17,18,28,29], in which above the CMC of SDS, the formed SDS micelles would redissolve the precipitated CDS. Furthermore, it could be found from the figure that with Ca^{2+} dosage being 7 mM and 9 mM, at 8 mM SDS dosage, the MB removal rates were both very high, which could reach 97.33% and 95.26%, respectively. This was probably attributed to that at the CMC value, the formed SDS micelles were capable of solubilizing the majority of MB molecules in the system, hence, under the effect of Ca^{2+} and MBFGA1, the most of MB molecules were removed in the form of CDS-MB particles. As a result, under 7 mM Ca^{2+} dosage, with SDS dosage varying from 8 mM to 12.6 mM, the MB removal efficiency increased from 97.33% to 98.82%, the increment was small; similarly, under 9 mM Ca^{2+} dosage, with SDS dosage varying from 8 mM to 16 mM, the MB removal efficiency also increased very slightly from 95.26% to 99.10%.

3.1.2. Influence of SDS dosage on the interaction between SDS and Ca^{2+}

The concentrations of MB and MBFGA1 were fixed at 50 mg/L and 4 mL/L, respectively. Under different Ca^{2+} dosages, the effects of SDS dosage on the Ca^{2+} concentration, SDS concentration in the upper liquid phase and the SDS removal efficiency were shown in Fig. 1(b) and (c). In Fig. 1(b), with the increment of SDS dosage, the Ca^{2+} concentration in the upper phase decreased to the minimum, followed by increasing significantly, and then reached a plateau. Obviously, the bottoms of the curves were the points that the redissolution of Ca^{2+} occurred as mentioned in Section 3.1.1. Taking the 5 mM Ca^{2+} dosage as an example, the point was at 12.6 mM SDS dosage. Actually, the redissolution of Ca^{2+} was probable due to the binding of Ca^{2+} in CDS particles onto the micelles formed in the upper liquid phase [28]. As the adsorption capacity of Ca^{2+} onto the micelles was higher than that of the Na^{+}, there existed ion-exchange phenomenon between Ca^{2+} and Na^{+} [16,17]. As a result, with the SDS dosage increasing from 12.6 to 48 mM, the SDS micelles in the upper liquid phase would adsorb the Ca^{2+} in CDS particles, resulting in the gradual dissolution of the CDS particles and the formation of SDS micelles containing the adsorbed Ca^{2+} in the upper liquid phase. Hence, the precipitated CDS particles acted as a reservoir for the supply of the Ca^{2+} to the micelles [17]. At 48 mM SDS dosage, the complete redissolution of Ca^{2+} occurred and the Ca^{2+} concentration in the upper phase resumed to the initial dosage. With the continuous increment of SDS dosage, the Ca^{2+} concentration in the upper phase kept constant.

As Fig. 1(c) illustrated, with the SDS dosage ranging from 1.4 to 80 mM, the SDS removal efficiency ascended to the maximum, and then descended to 0%. With Ca^{2+} dosages varying to be 5, 7 and 9 mM, the highest SDS removal efficiencies were achieved at 8, 12.6 and 16 mM SDS dosages, respectively. Correspondingly, at these critical points, the growth rates of the SDS concentrations

Table 2
Three dividing points of the reaction process under different Ca^{2+} dosages.

Ca^{2+} dosage (mM)	SDS dosage (mM)		
	Point 1	Point 2	Point 3
5	8	12.6	48
7	12.6	20	64
9	16	24	72

in the upper phase varied from slow to fast. Using the 5 mM Ca^{2+} dosage for example, this could be explained that when SDS dosage was below 8 mM, the reaction between SDS-MB monomers and Ca^{2+} prevailed in the system, so with the increment of the SDS dosage, the SDS removal efficiency kept ascending, and the SDS concentration in the upper phase increased very gently. However, at 8 mM SDS dosage, the resolubilization of MB by the SDS micelles in the upper liquid phase started to happen as elaborated in Section 3.1.1, which led to the decrease of the SDS removal efficiency and the steeper increment speed of the SDS concentration in the upper phase. In addition, it was noteworthy that the best SDS removal efficiency was about 90% at 8 mM SDS dosage, which indicated that the secondary pollution was very low.

When the Ca^{2+} dosage was fixed at 5 mM, the concentration consumptions of SDS and Ca^{2+} were plotted intuitively as columns in Fig. 1(d), meanwhile the concentration consumption ratio between SDS and Ca^{2+} was plotted as a line. From the figure, it was clear that the concentration consumption ratio between SDS and Ca^{2+} increased firstly, and then kept almost constant at a value of 2.0, which confirmed the viewpoint presented above that the reaction product between SDS monomers and Ca^{2+} was the calcium dodecyl sulfate $Ca(DS)_2$. Besides, when the SDS dosage was below 4.2 mM, the SDS-to-Ca^{2+} concentration consumption ratio was less than 2.0, probably because the formed $Ca(DS)_2$-MB particles would adsorb the redundant Ca^{2+} in the upper phase.

In a word, based on the analysis in Section 3.1, as the SDS dosage increased, the reaction process in the system could be divided by three points denoted 1, 2 and 3. At point 1, the highest MB and SDS removal efficiencies could be achieved, and the resolubilization of MB adsorbed on the $Ca(DS)_2$ particles occurred. The point 2 represented the beginning of the redissolution of Ca^{2+} in the $Ca(DS)_2$-MB particles. At point 3, the $Ca(DS)_2$-MB particles in flocs were dissolved completely and the clear blue solution appeared. Under different Ca^{2+} dosages of 5, 7, 9 mM, the three dividing points were shown in Table 2.

3.2. Effects of Ca^{2+} dosage

3.2.1. Influence of Ca^{2+} dosage on the MB removal

The concentrations of MB and MBFGA1 were 50 mg/L and 4 mL/L, respectively. In Fig. 2(a), as the SDS dosages varied to be 8, 12

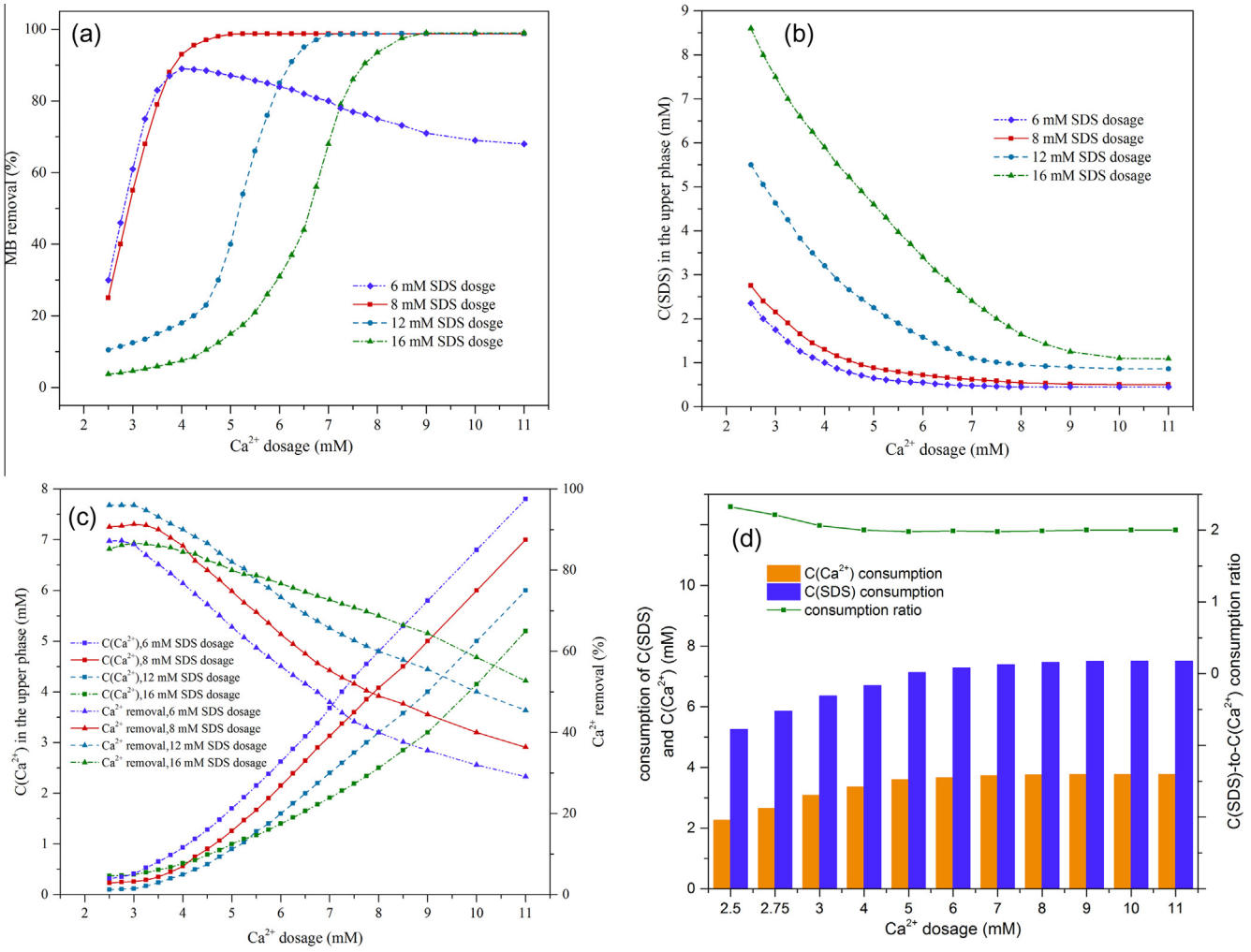

Fig. 2. Effects of Ca^{2+} dosage on the (a) MB removal efficiency, (b) SDS concentration in the upper phase, (c) Ca^{2+} concentration in the upper phase and Ca^{2+} removal efficiency at different SDS dosages of 6, 8, 12, and 16 mM; (d) SDS and Ca^{2+} concentration consumption and SDS-to-Ca^{2+} concentration consumption ratio at 8 mM SDS dosage. The MB concentration and MBFGA1 dosage were 50 mg/L and 4 mL/L, respectively.

and 16 mM, the variation trends of MB removal efficiencies with Ca^{2+} dosage were in similar pattern. That was the MB removal efficiencies ascended significantly, and then reached a platform with Ca^{2+} dosage increasing from 2.5 to 11 mM. When the Ca^{2+} dosage was low, the Ca^{2+} would be adsorbed onto the SDS-MB micelles in the solution because the micelles had a number of binding sites for Ca^{2+} [28], and the association of the micelles with Ca^{2+} was preferential over the association with Na^{+} [16,17]. With the Ca^{2+} dosage increasing, the Ca^{2+} would start to react with the SDS-MB monomers gradually to generate $Ca(DS)_2$-MB particles. As the Ca^{2+} dosage continued to rise, under the effect of Ca^{2+}, SDS-MB micelles would disassemble gradually into the SDS-MB monomers and the CDS-MB particles formed continually. Finally, the CDS-MB particles were flocculated by MBFGA1, and the MB removal efficiency reached the maximum of 98.63%, 98.82% and 99.10% at 5, 7 and 9 mM Ca^{2+} dosages under SDS dosages of 8, 12 and 16 mM, respectively. This was in accordance with the results shown in Fig. 1(a).

However, from Fig. 2(a), when SDS dosage was 6 mM, the variation trend of MB removal efficiency with Ca^{2+} dosage was different from the other three curves. As Ca^{2+} dosage increased from 2.5 to 11 mM, the MB removal efficiency ascended firstly, and then descended. The highest removal rate reached 89% at 4 mM Ca^{2+} dosage. This phenomenon was probably attributed to that when SDS concentration was 6 mM, though it was lower than the CMC of SDS, the SDS molecules could form small premicelles which were able to provide MB with a micelle-like environment and solubilize a portion of MB molecules in the system [10,24,25]. Therefore, with the Ca^{2+} dosage increasing, the SDS-MB premicelles would disassemble gradually into the SDS-MB monomers, and the CDS-MB particles formed continually. However, it was worth noting that in the SDS premicelles, the interaction between SDS and MB was mainly electrostatic attraction, the hydrophobic interaction was weak, which was probably due to the normal micelles have not been formed [24,25,30]. In addition, excessive Ca^{2+} may weaken the electrostatic interaction between SDS and MB, and thus reducing the amount of MB associated with SDS in the premicellar region. Therefore, above the 4 mM, further increase of Ca^{2+} dosage led to the decrease of MB removal efficiency.

3.2.2. Influence of Ca^{2+} dosage on the interaction between SDS and Ca^{2+}

Under different SDS dosages of 6, 8, 12 and 16 mM, the effects of Ca^{2+} dosage on the Ca^{2+} concentration, SDS concentration in the upper liquid phase and the Ca^{2+} removal efficiency were illustrated in Fig. 2(b) and (c). From Fig. 2(b), as Ca^{2+} dosage varied from 2.5 to 11 mM, the SDS concentration in the upper phase decreased gradually, and remained constant eventually. This variation trend was due to the reaction between Ca^{2+} and SDS-MB monomers as stated in Section 3.2.1. However, taking 8 mM SDS dosage to elaborate,

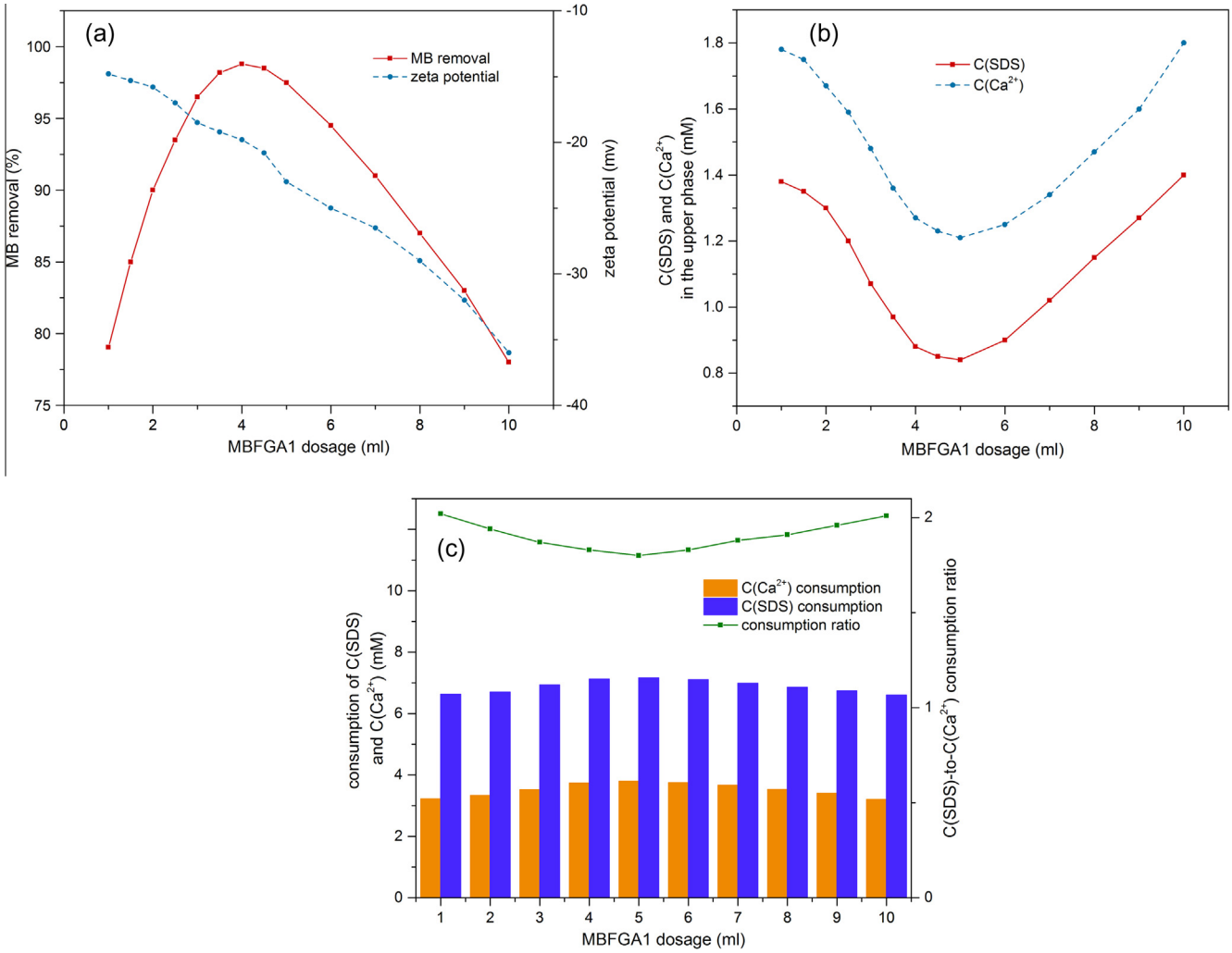

Fig. 3. Effects of MBFGA1 dosage on the (a) MB removal efficiency, (b) SDS and Ca^{2+} concentration in the upper phase, (c) SDS and Ca^{2+} concentration consumption and SDS-to-Ca^{2+} concentration consumption ratio. The MB concentration, SDS and Ca^{2+} dosage were 50 mg/L, 8 mM and 5 mM, respectively.

after the best MB removal rate was achieved at 5 mM Ca^{2+} dosage, the SDS concentration in the upper phase continued to descend with the Ca^{2+} dosage increasing. This was possibly because there was a small amount of SDS residual in the upper liquid phase, which would continue to react with Ca^{2+} after the SDS-MB micelles were consumed completely by Ca^{2+}. In addition, it was noteworthy that at 6 mM SDS dosage, while the interaction between SDS and MB was lowered by the excessive Ca^{2+} dosage, there was no influence on the reaction between SDS and Ca^{2+}.

In Fig. 2(c), the Ca^{2+} concentration in the upper phase ascended with Ca^{2+} dosage, varying from slightly to quickly. Correspondingly, the variation of Ca^{2+} removal efficiency changed from ascent to descent. When the SDS dosages were 8, 12 and 16 mM, the critical points were all at 3 mM Ca^{2+} dosage. Taking the 8 mM SDS dosage to explain, below the 3 mM, a portion of Ca^{2+} were bonded to the SDS-MB micelles in the upper phase while a small quantity of $Ca(DS)_2$-MB particles had been generated. Based on the experimental phenomenon, the SDS-MB micelles containing the adsorbed Ca^{2+} formed very finely dispersed sols in the upper phase [31]. As mentioned in Section 2.3, the water samples should be filtered through 0.45 μm filter membrane before the concentration measurements of SDS and Ca^{2+} were taken, hence, the dispersed sols would be filtered out and in turn the remnant calcium ions in the filtrate were measured. Therefore, when Ca^{2+} dosage was lower than 3 mM, the growth rate of the Ca^{2+} concentration in the upper phase was low and the Ca^{2+} removal efficiency increased gradually. As Ca^{2+} dosage ascended from 3 to 9 mM, the main behavior of Ca^{2+} was reacting with SDS-MB monomers (or SDS monomers) to form $Ca(DS)_2$-MB particles (or $Ca(DS)_2$ particles) and the sols dispersed in the upper phase disappeared, hence filtration had no influence on the Ca^{2+} concentration in the upper phase. Therefore, the growth rate of Ca^{2+} concentration in the upper phase changed from low to high and the Ca^{2+} removal efficiency changed to descend. With the continuous increment of Ca^{2+} dosage to 11 mM, the Ca^{2+} concentration in the upper phase increased more sharply, and the concentration consumptions of Ca^{2+} and SDS kept constant as shown in Fig. 2(d). This indicated that the reaction between SDS and Ca^{2+} had been proceeded completely at 9 mM Ca^{2+} dosage, which was consistent with the results presented in Fig. 2(b). However, from Fig. 2(c), it could be found that when SDS dosage was 6 mM, the critical point was at 2 mM Ca^{2+} dosage, which was smaller than that at the other three SDS dosages. This was possibly attributed to that the premicelles formed at 6 mM SDS dosage had lower adsorption capacity for Ca^{2+} than the normal micelles, hence, the sols disappeared at lower Ca^{2+} dosage, accordingly, the critical point was smaller.

When the SDS dosage was fixed at 8 mM, the variations of the concentration consumptions of SDS and Ca^{2+}, and SDS-to-Ca^{2+} consumption ratio with Ca^{2+} dosage were displayed in Fig. 2(d). It was clear that the SDS-to-Ca^{2+} consumption ratio was more than 2.0 when Ca^{2+} dosage was below 3 mM. This phenomenon was possibly due to the dispersed sols in the upper phase which was mainly comprised of SDS-MB micelles containing the adsorbed Ca^{2+} (SDS-MB/Ca^{2+} micelles). In the SDS-MB/Ca^{2+} micelles, the concentration ratio between SDS and Ca^{2+} was more than 2.0, hence the SDS-to-Ca^{2+} consumption ratio in the system was above 2.0 as the sols were filtrated. When Ca^{2+} dosage was above 3 mM, the sols disappeared and the reaction to generate $Ca(DS)_2$ prevailed in the system, so the SDS-to-Ca^{2+} consumption ratio turned to 2.0.

Table 4
CCD design and response values.

Run	Factors			Response
	x_1 (mM)	x_2 (mM)	x_3 (mL/L)	MB removal efficiency (%)
1	8	5	4	98.31
2	8	5	0.64	60
3	4	7	6	90
4	8	1.64	4	41.99
5	8	5	4	98.33
6	8	5	4	98.74
7	12	7	6	92
8	4	3	2	47.40
9	8	8.36	4	90
10	12	3	6	27
11	12	7	2	98
12	4	7	2	44
13	14.73	5	4	25
14	8	5	4	98.01
15	1.27	5	4	60
16	8	5	7.36	70
17	8	5	4	98.04
18	8	5	4	98.53
19	12	3	2	29
20	4	3	6	43.66

Table 5
Analysis of variance (ANOVA) for the quadratic model.

Source	Sum of squares	Degrees of freedom	Mean square	F-value	P-value Prob > F
Model	14127.09	9	1569.68	13.39	0.0002
X_1	105.29	1	105.29	0.90	0.3656
X_2	4862.03	1	4862.03	41.47	<0.0001
X_3	191.01	1	191.01	1.63	0.2307
X_1X_2	1036.41	1	1036.41	8.84	0.0140
X_1X_3	315.71	1	315.71	2.69	0.1318
X_2X_3	261.56	1	261.56	2.23	0.1661
X_1^2	5201.10	1	5201.10	44.36	<0.0001
X_2^2	1646.96	1	1646.96	14.05	0.0038
X_3^2	1757.28	1	1757.28	14.99	0.0031
Residual	1172.38	10	117.24	–	–
Lack of fit	1171.98	5	234.40	2997.05	<0.0001
Pure error	0.39	5	0.078	–	–

Standard Deviation = 10.83, R^2 = 0.9234, R^2_{adj} = 0.8544.

3.3. Effects of MBFGA1 dosage

Based on the analysis in Sections 3.1 and 3.2, it could be concluded that in the MB removal process, the major role that MBFGA1 played was to flocculate the CDS-MB particles. Therefore, when investigating the effects of MBFGA1, it was important to make the majority of MB molecules precipitate from the aqueous solution by adsorbing onto the CDS particles. So, considering the effect and the economy in the MB removal process, the 8 mM

Table 3
Various methods used for the removal of MB and SDS.

Method	MB concentration (mg/L)	MB removal efficiency (%)	Removal capacity (mg/L)	SDS concentration (mM)	SDS removal efficiency (%)	Refs.
This work	50	98.63	49.32	8	88.97	
MEUF	6	99.3	5.96	8	63.48	[1]
MEUF	5	94.33	4.72	40	Unstudied	[8]
Adsorption	5	91	4.55	1	Unstudied	[4]
Adsorption	50	85.2	42.6	1	Unstudied	[5]

Table 6
Significance of quadratic model coefficient.

Factor	Regression coefficients	Degrees of freedom	Standard error	Prob > F
Intercept	98.21	1	4.42	–
X_1	−2.78	1	2.93	0.3656
X_2	18.87	1	2.93	<0.0001
X_3	3.74	1	2.93	0.2307
X_1X_2	11.38	1	3.83	0.0140
X_1X_3	−6.28	1	3.83	0.1318
X_2X_3	5.72	1	3.83	0.1661
X_1^2	−19.00	1	2.85	<0.0001
X_2^2	−10.69	1	2.85	0.0038
X_3^2	−11.04	1	2.85	0.0031

SDS dosage and 5 mM Ca^{2+} dosage were adopted as the research dosage in this Section.

3.3.1. Influence of MBFGA1 dosage on flocculation behavior

The effect of MBFGA1 dosage on the flocculation of $Ca(DS)_2$-MB particles was investigated when the MB concentration, the dosages of SDS and Ca^{2+} were fixed at 50 mg/L, 8 mM and 5 mM, respectively. Fig. 3(a) showed the evolutions of MB removal efficiency and zeta potential of the supernatant with MBFGA1 dosage ranging from 1 to 10 mL. As could be seen from Fig. 3(a), the MB removal efficiency increased at the beginning and then decreased with increasing addition of MBFGA1. The maximum removal efficiency reached about 99% when 4 mL MBFGA1 was added. This demonstrated that a higher MBFGA1 dosage could adsorb more CDS-MB particles to form lager flocs. However, above the 4 mL, further increase of MBFGA1 led to the well-known re-stabilization phenomenon [19,32]. It was attributed to that there were more negative charges in the excessive MBFGA1 solution, which caused the stronger charge repulsion and inhibited small flocs to grow into big ones.

On the other hand, as shown in Fig. 3(a), the zeta potential always decreased with the increase of MBFGA1 dosage and was less than zero at any dosage, which was due to the negative zeta potential of MBFGA1 [19,33] and CDS-MB particles. In addition, it could be seen that the best MB removal efficiency was achieved at a zeta potential of about −20 mv, which meant that adsorption bridging through repulsive obstacle played a major role during the flocculation process [19,32]. In the process, MBFGA1 acted as a bridging reagent of many small aggregates adsorbed CDS-MB particles. These aggregates could form larger flocs by the bridging mechanism, and precipitate as evidenced in the jar tests. Meanwhile, many CDS-MB particles could be adsorbed onto a long molecular chain of MBFGA1, and the particles adsorbed on the chain could be adsorbed simultaneously by other MBFGA1 chains. Thus, the three-dimensional flocs formed with a better settling

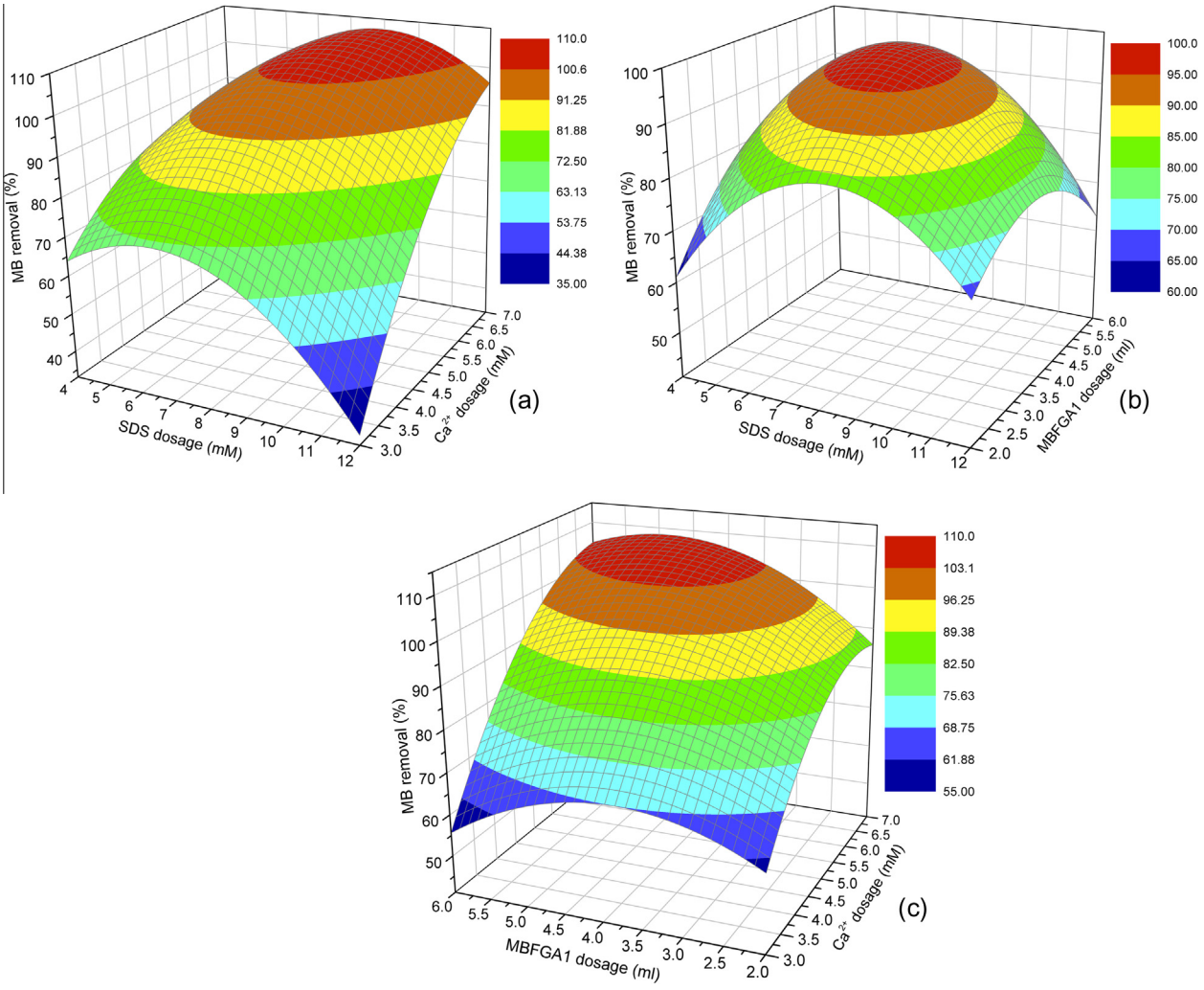

Fig. 4. Surface graphs of MB removal efficiency showing the effect of variables: (a) SDS dosage and Ca^{2+} dosage (b) SDS dosage and MBFGA1 dosage (c) Ca^{2+} dosage and MBFGA1 dosage.

capacity [32]. Furthermore, the calcium ions in the CDS-MB particles could probably promote the flocculation by reducing the electrostatic repulsion between anionic polymers and negatively-charged colloidal particles, and making MBFGA1 attract more CDS-MB particles around its surface [19,23]. The calcium ions had also been reported to develop bridges between anionic polymers and negatively-charged colloidal particles, thereby enhancing particle flocculation [34].

3.3.2. Influence of MBFGA1 dosage on the interaction between SDS and Ca^{2+}

The effect of MBFGA1 dosage on the interaction between SDS and Ca^{2+} was illustrated in Fig. 3(b) and (c) when MB concentration, the dosages of SDS and Ca^{2+} were fixed at 50 mg/L, 8 mM and 5 mM, respectively. As shown in Fig. 3(b), the variation trends of the concentrations of SDS and Ca^{2+} in the upper phase with MBFGA1 dosage were in similar pattern. The two curves were like the upward parabolas and the lowest values were both achieved at MBFGA1 dosage of 5 mL. Nevertheless, as mentioned in Section 2.3, the water samples should be filtered through 0.45 μm filter membrane before the concentration measurements of SDS and Ca^{2+} were taken. It was worth noting that the formed CDS-MB particles could be filtered out completely even if MBFGA1 was not added. The reason why the concentrations of SDS and Ca^{2+} in the upper phase varied with MBFGA1 dosage was possible that MBFGA1 could adsorb Ca^{2+} residual in the supernatant [19,23] after the most of CDS-MB particles had been generated, leading to the Ca^{2+} concentration polarization phenomenon on the MBFGA1. When reached to a certain value, the Ca^{2+} aggregated on the MBFGA1 would then react with SDS monomers residual in the supernatant to form $Ca(DS)_2$. These $Ca(DS)_2$ particles was also binded to the adsorption sites of MBFGA1 and thereby being flocculated by the adsorption bridging mechanism. In conclusion, during the process, the added MBFGA1 could not only flocculate the previously generated CDS-MB particles, but also facilitate the reaction between SDS and Ca^{2+} remnant in the supernatant because of concentration polarization effect, which in turn improved the SDS removal efficiency and led to the lower secondary pollution.

In Fig. 3(c), with GA1 dosage increasing from 1 to 10 mL, the SDS-to-Ca^{2+} consumption ratio decreased firstly from 2.0 to 1.8 at 5 mL MBFGA1 dosage, and then returned to 2.0. The variation trend of the SDS-to-Ca^{2+} consumption ratio was similar to the curves in Fig. 3(b). Obviously, the SDS-to-Ca^{2+} consumption ratio was also influenced by the concentration polarization effect of MBFGA1. The reason why the ratio was less than 2.0 in the process was possible that the calcium ions adsorbed on the MBFGA1 were excessive and could not completely enter into the reaction with SDS monomers in the supernatant.

All in all, according to the analysis in Sections 3.1–3.3, considering the MB removal efficiency, secondary pollution, and economy in the reaction process, the optimal conditions were SDS 8 mM, Ca^{2+} 5 mM and MBFGA1 4 mL/L, respectively, which were also determined as the central value of the central composite design in Section 3.4. Table 3 showed the removal efficiency of MB and SDS under the optimal conditions compared with other methods studied previously. From Table 3, it could be seen that the MB removal capacity and the SDS removal efficiency were both high using the approach proposed in this study, which indicated that

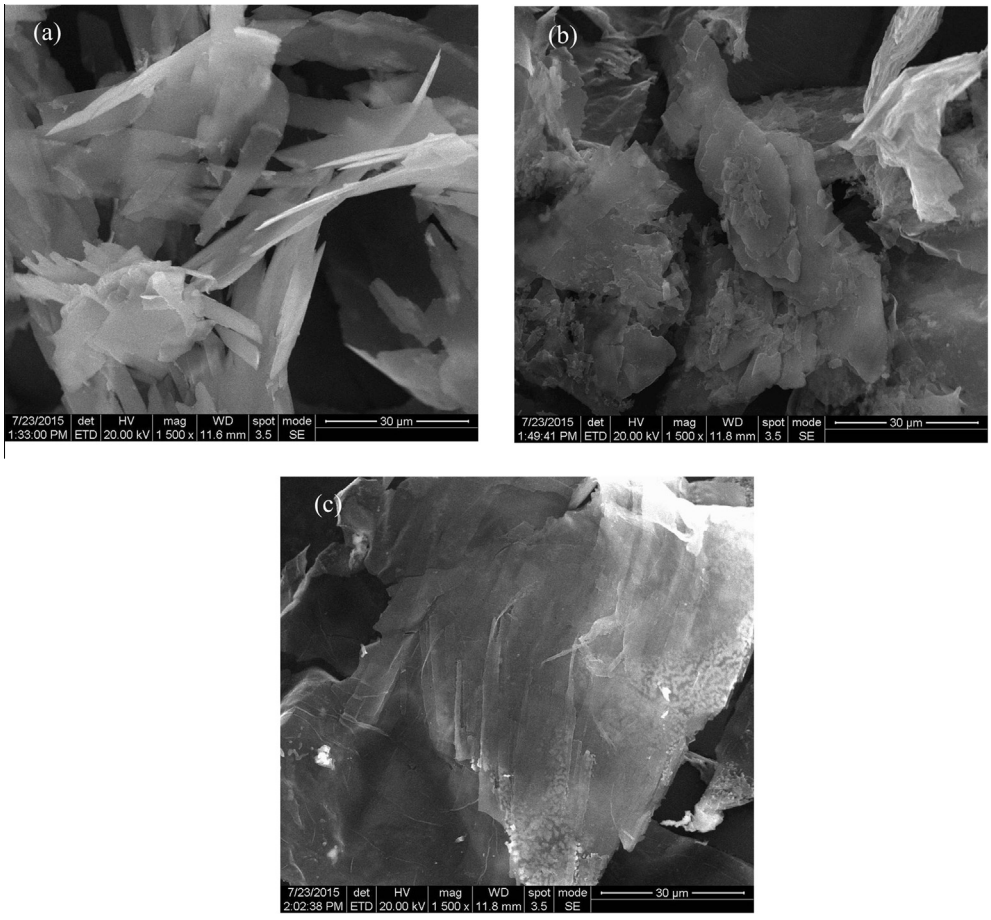

Fig. 5. ESEM images of flocs formed under different SDS dosages: (a) 8 mM, 1500× (b) 16 mM, 1500× (c) 24 mM, 1500×. The MB concentration, Ca^{2+} and MBFGA1 dosage were 50 mg/L, 5 mM and 4 mL/L, respectively.

this approach was high efficient, eco-friendly and widely applicable.

3.4. Response surface methodology of reaction factors

To further explore the interactive effects of independent variables on the MB removal efficiency, CCD was employed. The response variables of MB removal efficiency acquired from 20 groups of experiments were shown in Table 4. According to the experimental results, the best second-order polynomial equation in terms of coded factors was obtained as follows:

$$Y = +98.21 - 2.78x_1 + 18.87x_2 + 3.74x_3 + 11.38x_1x_2 - 6.28x_1x_3 + 5.72x_2x_3 - 19.00x_1^2 - 10.69x_2^2 - 11.04x_3^2 \quad (7)$$

The statistical testing of this model was performed with the Fish's statistical method for analysis of variance (ANOVA). The result of ANOVA, shown in Table 5, indicated that the second-order equation fitted well. Because model value of 'Prob > F' = 0.0002 was less than 0.05, the total determination coefficient R^2 reached 0.9234, and the adjusted R^2 values were 0.8544. Among them, R^2 indicated the percentage of experimental data that were compatible with the model, R^2_{adj} indicated the fraction of variation of the response explained by the model.

The significance testing for the coefficient of the Eq. (7) was listed in Table 6. Values of 'Prob > F' less than 0.05 indicated model terms were significant. In the linear terms, the Ca^{2+} dosage was significant. Undoubtedly, when Ca^{2+} dosage was inadequate, the reaction between SDS-MB monomers and Ca^{2+} could not proceed thoroughly, accordingly, the MB removal efficiency was low. Only when Ca^{2+} dosage was sufficient relatively, the majority of MB molecules could precipitate from the aqueous solution by adsorbing onto the CDS particles, hence, MB could be removed effectively. Therefore, the Ca^{2+} dosage played an important role in the MB removal process. Among the higher order effects, the quadratic terms of SDS dosage, Ca^{2+} dosage and MBFGA1 dosage were all significant. The interaction terms were presented in Fig. 4. Fig. 4(a) showed the change of MB removal efficiency with the dosage of SDS and Ca^{2+} varying, while the dosage of MBFGA1 was kept at central level. The figure indicated that the interactive effects between SDS and Ca^{2+} on MB removal efficiency were significant. At a low level of Ca^{2+}, only a small quantity of SDS dosage were needed to remove MB significantly, excessive SDS dosage could even reduce the MB removal efficiency. However, when Ca^{2+} dosage was high, more quantity SDS dosages should be added to reach the highest MB removal efficiency. This conclusion was very consistent with the viewpoint put forward in Section 3.1 and ver-

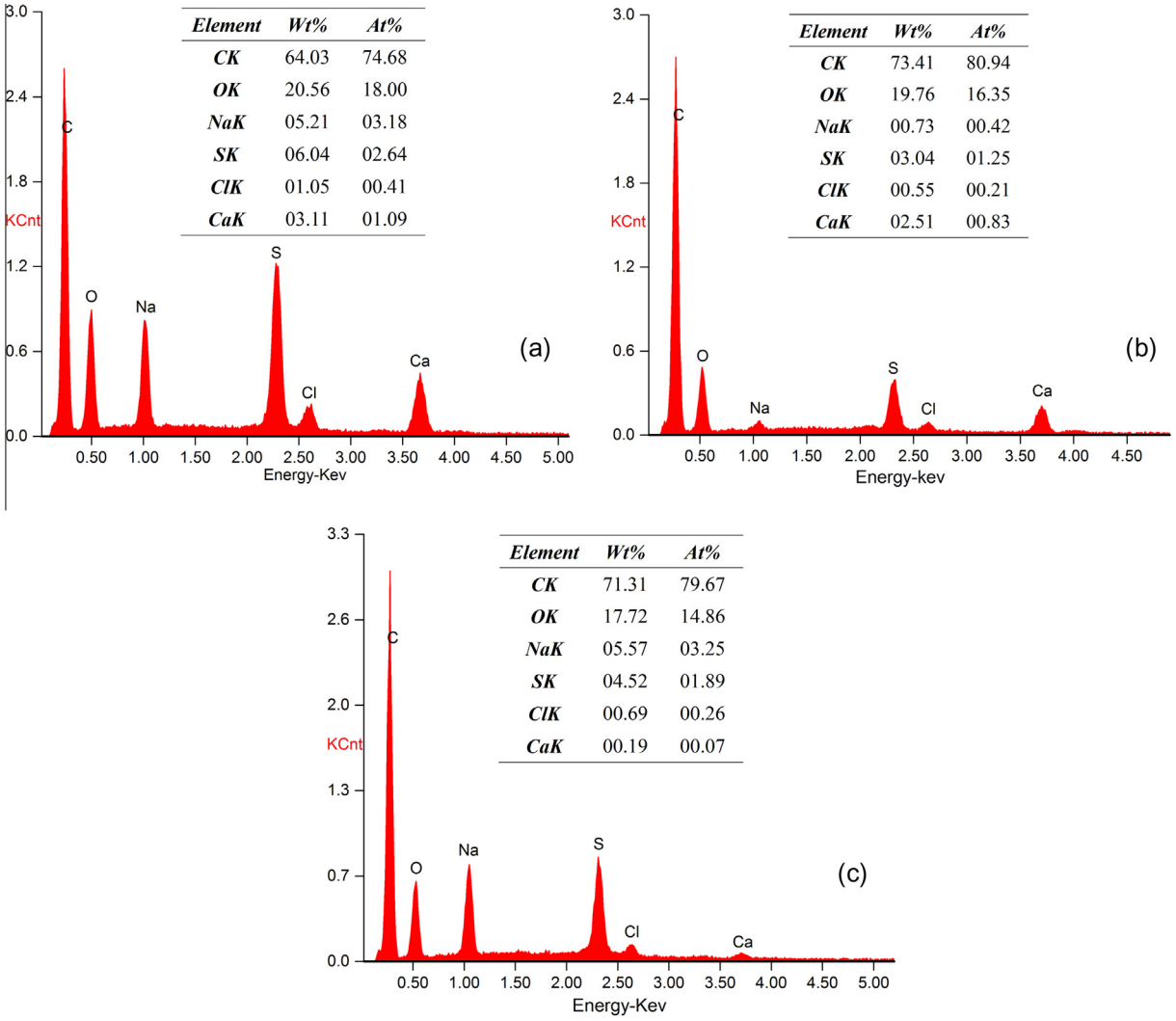

Fig. 6. EDS spectras of flocs formed under different SDS dosages: (a) 8 mM (b) 16 mM (c) 24 mM. The MB concentration, Ca^{2+} and MBFGA1 dosage were 50 mg/L, 5 mM and 4 mL/L, respectively.

ified the analysis about the interaction between SDS and Ca^{2+} in Section 3.1. Fig. 4(b) and (c) both indicated that MBFGA1 had obvious quadratic effect on the MB removal efficiency in reaction process when another factor was at central level.

According to the target value of 100% MB removal efficiency, the optimum conditions calculated from the regression equations were SDS 8.2 mM, Ca^{2+} 5.3 mM, and MBFGA1 4.5 mL/L, respectively. The removal efficiency of verification test operated under the optimum conditions was greater than 99%. However, considering the economy in the reaction process, the conditions of SDS 8 mM, Ca^{2+} 5 mM, and MBFGA1 4 mL/L were still regarded as the optimal conditions.

3.5. Environmental scanning electron microscope analysis

When MB concentration, the dosage of Ca^{2+} and MBFGA1 were fixed at 50 mg/L, 5 mM and 4 mL/L, respectively, under different SDS dosages of 8, 16, 24 mM, the corresponding ESEM micrographs of formed flocs were displayed in Fig. 5. Fig. 5(a) showed the flocs formed at the optimal conditions had loose and strip structure, and smooth surface morphology. With the SDS dosage increasing, the generated flocs, as shown in Fig. 5(b), became compact and massive texture, and tough surface morphology. When the SDS dosage ascended to 24 mM, the flocs presented in Fig. 5(c) had denser and larger blocky structure, which indicated that with the redissolution of CDS-MB particles, the combination force between SDS and Ca^{2+} in flocs became stronger.

Energy dispersive spectrometer (EDS) was used to analyze the elemental composition of the flocs formed under three different conditions as stated above. Obviously, the signal value of Ca peak weakened gradually as the SDS dosage increased in Fig. 6, probably resulting from the redissolution of Ca^{2+}. Thus, EDS analysis gave puissant supports to previous experimental results.

3.6. Interaction mechanism between SDS and Ca^{2+} and MB removal mechanism

Based on the above results and discussion, the interaction mechanism between SDS and Ca^{2+} and MB removal mechanism were schematically described in Fig. 7.

3.6.1. Interaction mechanism between SDS and Ca^{2+}

When SDS concentration was equal to or higher than its CMC, the SDS monomers would assemble to form micelles which could solubilize MB molecules [1]. Hence, the formed SDS micelles containing the solubilized MB (SDS-MB micelles) kept dynamic equi-

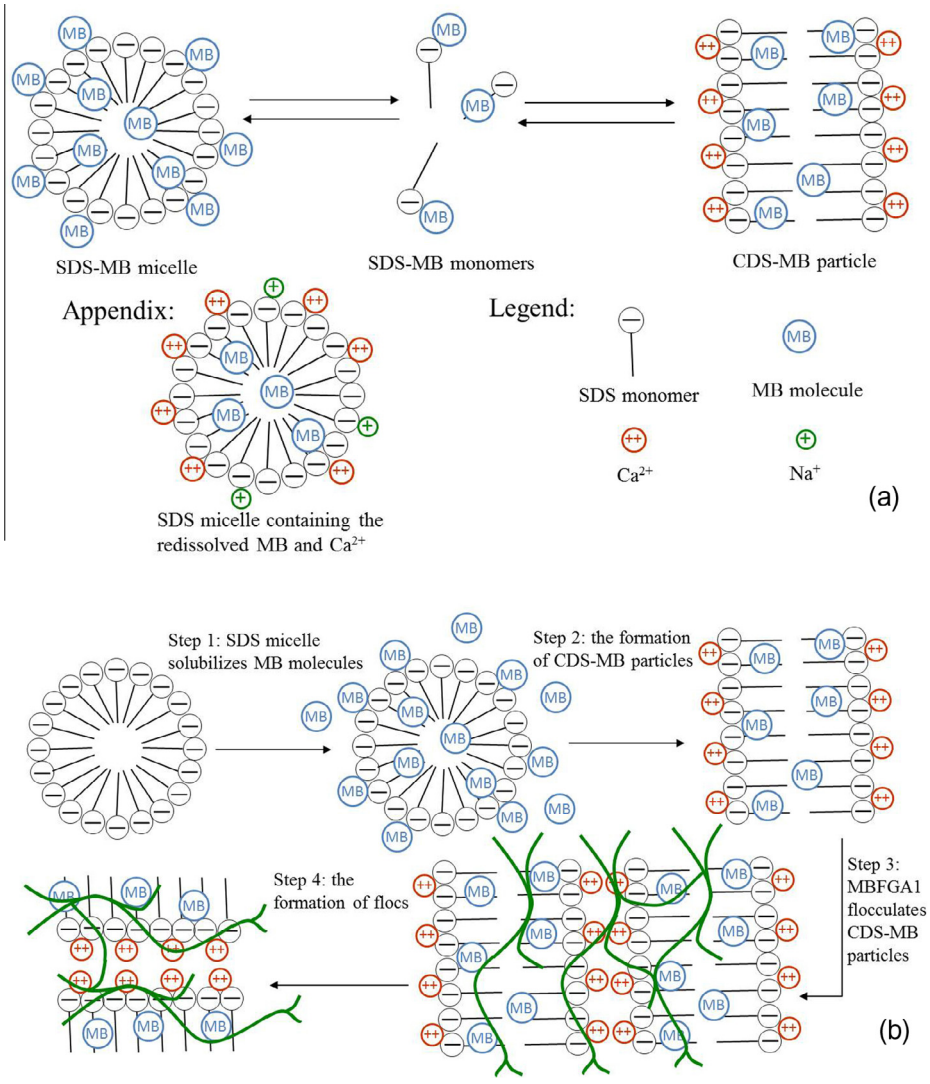

Fig. 7. Schematic diagrams: (a) equilibrium in the reaction process and SDS micelle containing the redissolved MB and Ca^{2+} (b) suggested MB removal mechanism.

librium with the SDS monomers adsorbed MB (SDS-MB monomers) [17]. Meanwhile, the Ca^{2+} in the system would react with the SDS-MB monomers to generate MB loaded calcium dodecyl sulfate (CDS) particles (CDS-MB particles) [16–18]. Therefore, in the system, SDS-MB micelles, SDS-MB monomers and CDS-MB particles coexisted and maintained dynamic equilibrium as displayed in Fig. 7(a) [17].

When Ca^{2+} concentration was relatively sufficient compared to the SDS concentration in the system, the equilibrium in Fig. 7(a) would be shifted toward the right, resulting in the gradual disassembly of SDS-MB micelles and the formation of CDS-MB particles. However, when SDS concentration was relatively excessive and SDS micelles had been formed in the upper liquid phase at levels equal to or higher than 1 CMC, the equilibrium in Fig. 7(a) would be shifted toward the left, which was due to the association of SDS micelles in the upper liquid phase with MB and Ca^{2+} in the CDS-MB particles [16,18]. As a result, the precipitated CDS-MB particles in flocs dissolved, and SDS micelles containing the redissolved MB and Ca^{2+} in the upper liquid phase formed gradually as presented in Fig. 7(a).

Based on the analysis stated above, it could be concluded that the interaction between SDS and Ca^{2+} was depended heavily on the SDS-Ca^{2+} concentration ratio in aqueous solution, rather than the CMC of SDS. This conclusion advanced the former research results [17,18,28,29], which showed that the interaction between SDS and Ca^{2+} was only related to the CMC of SDS.

3.6.2. MB removal mechanism

When Ca^{2+} concentration was relatively sufficient in the system, the equilibrium in Fig. 7(a) would be shifted toward the right, and CDS-MB particles formed continually due to the reaction between SDS-MB monomers and Ca^{2+}. Therefore, MB precipitated from aqueous solution by adsorbing onto the CDS particles. Finally, the suspended CDS particles adsorbed MB were flocculated by MBFGA1. Clearly, the highest MB removal efficiency was achieved when the reaction between SDS monomers and Ca^{2+} had been proceeded thoroughly. The schematic diagram of the MB removal process was shown in Fig. 7(b).

4. Conclusions

A novel approach was proposed for the removal of MB from aqueous solution by $Ca(DS)_2$ enhanced precipitation and MBFGA1 flocculation. In this approach, the solubility of MB was innovatively reduced by the combination of the solubilization effect of SDS on MB and the calcium ion effect on SDS-MB micelles. Under the optimal conditions of pH (10), MB (50 mg/L), SDS (8 mM), Ca^{2+} (5 mM) and MBFGA1 (4 mL/L), the removal efficiency of MB and SDS could achieve 98.63% and 88.97%, respectively, which indicated that this approach was simple, high efficient, eco-friendly and cost-effective. The research results also showed that the interaction between SDS and Ca^{2+} was closely related to the SDS-Ca^{2+} concentration ratio in aqueous solution rather than the CMC of SDS, which advanced the former viewpoints and was of instructive significance to the other organic pollutants removal by this method in the future. In conclusion, the approach proposed in this study was promising for the real MB wastewater purification due to its efficiency and economic feasibility, in addition, it could be extended to other surfactants and organic pollutants even heavy metals in theory, which need more studies in the future to broaden its applications.

Acknowledgement

This study was sponsored by the National Natural Science Foundation of China (Grants No. 51378189, 51578223 and 51521006).

Appendix A. Supplementary data

Supplementary data associated with this article can be found, in the online version, at http://dx.doi.org/10.1016/j.cej.2016.05.101.

References

[1] J.-H. Huang, C.-F. Zhou, G.-M. Zeng, X. Li, J. Niu, H.-J. Huang, L.-J. Shi, S.-B. He, Micellar-enhanced ultrafiltration of methylene blue from dye wastewater via a polysulfone hollow fiber membrane, J. Membr. Sci. 365 (2010) 138–144.
[2] Z. Wu, H. Zhong, X. Yuan, H. Wang, L. Wang, X. Chen, G. Zeng, Y. Wu, Adsorptive removal of methylene blue by rhamnolipid-functionalized graphene oxide from wastewater, Water Res. 67 (2014) 330–344.
[3] A.Y. Zahrim, C. Tizaoui, N. Hilal, Coagulation with polymers for nanofiltration pre-treatment of highly concentrated dyes: a review, Desalination 266 (2011) 1–16.
[4] R. Abdallah, S. Taha, Biosorption of methylene blue from aqueous solution by nonviable *Aspergillus fumigatus*, Chem. Eng. J. 195–196 (2012) 69–76.
[5] Z. Aksu, S. Ertugrul, G. Donmez, Methylene blue biosorption by *Rhizopus arrhizus*: effect of SDS (sodium dodecylsulfate) surfactant on biosorption properties, Chem. Eng. J. 158 (2010) 474–481.
[6] Ö. Kerkez-Kuyumcu, E. Kibar, K. Dayıoğlu, F. Gedik, A.N. Akın, Ş. Özkara-Aydınoğlu, A comparative study for removal of different dyes over M/TiO_2 (M = Cu, Ni Co, Fe, Mn and Cr) photocatalysts under visible light irradiation, J. Photochem. Photobiol. A Chem. 311 (2015) 176–185.
[7] S.A. Ong, E. Toorisaka, M. Hirata, T. Hano, Biodegradation of redox dye methylene blue by up-flow anaerobic sludge blanket reactor, J. Hazard. Mater. 124 (2005) 88–94.
[8] M. Bielska, J. Szymanowski, Removal of methylene blue from waste water using micellar enhanced ultrafiltration, Water Res. 40 (2006) 1027–1033.
[9] G.M. Zeng, X. Li, J.H. Huang, C. Zhang, C.F. Zhou, J. Niu, L.J. Shi, S.B. He, F. Li, Micellar-enhanced ultrafiltration of cadmium and methylene blue in synthetic wastewater using SDS, J. Hazard. Mater. 185 (2011) 1304–1310.
[10] J.-H. Huang, C.-F. Zhou, G.-M. Zeng, X. Li, H.-J. Huang, J. Niu, F. Li, L.-J. Shi, S.-B. He, Studies on the solubilization of aqueous methylene blue in surfactant using MEUF, Sep. Purif. Technol. 98 (2012) 497–502.
[11] P.J. Quinlan, A. Tanvir, K.C. Tam, Application of the central composite design to study the flocculation of an anionic azo dye using quaternized cellulose nanofibrils, Carbohydr. Polym. 133 (2015) 80–89.
[12] M. Riera-Torres, C. Gutiérrez-Bouzán, M. Crespi, Combination of coagulation–flocculation and nanofiltration techniques for dye removal and water reuse in textile effluents, Desalination 252 (2010) 53–59.
[13] Y. Anjaneyulu, N. Sreedhara Chary, D. Samuel Suman Raj, Decolourization of industrial effluents – available methods and emerging technologies – a review, Rev. Environ. Sci. Biotechnol. 4 (2005) 245–273.
[14] S. Chatterjee, T. Chatterjee, S.R. Lim, S.H. Woo, Adsorption of a cationic dye, methylene blue, on to chitosan hydrogel beads generated by anionic surfactant gelation, Environ. Technol. 32 (2011) 1503–1514.
[15] R. Ansari, B. Seyghali, A. Mohammad-khah, M.A. Zanjanchi, Application of nano surfactant modified biosorbent as an efficient adsorbent for dye removal, Sep. Sci. Technol. 47 (2012) 1802–1812.
[16] M. Baviere, B. Bazin, R. Aude, Calcium effect on the solubility of sodium dodecyl sulfate in sodium chloride solutions, J. Colloid Interface Sci. 92 (1983) 580–583.
[17] R. Kumar, S. Bhat, Studies on surface activity of linear alkylbenzene sulfonates II: effect of water hardness, J. Am. Oil Chem. Soc. 64 (1987) 556–561.
[18] J. Peacock, E. Matijević, Precipitation of alkylbenzene sulfonates with metal ions, J. Colloid Interface Sci. 77 (1980) 548–554.
[19] J. Feng, Z. Yang, G. Zeng, J. Huang, H. Xu, Y. Zhang, S. Wei, L. Wang, The adsorption behavior and mechanism investigation of Pb(II) removal by flocculation using microbial flocculant GA1, Bioresour. Technol. 148 (2013) 414–421.
[20] Z.H. Yang, Z. Wu, G.M. Zeng, J. Huang, H.Y. Xu, J. Feng, P.P. Song, M. Li, L.k. Wang, Assessing the effect of flow fields on flocculation of kaolin suspension using microbial flocculant GA1, RSC Adv. 4 (2014) 40464–40473.
[21] J. Huang, Z.-H. Yang, G.-M. Zeng, M. Ruan, H.-Y. Xu, W.-C. Gao, Y.-L. Luo, H.-M. Xie, Influence of composite flocculant of PAC and MBFGA1 on residual aluminum species distribution, Chem. Eng. J. 191 (2012) 269–277.
[22] M.J. Rosen, J.T. Kunjappu, Surfactants and Interfacial Phenomena, John Wiley & Sons, 2012.
[23] Z.-H. Yang, J. Huang, G.-M. Zeng, M. Ruan, C.-S. Zhou, L. Li, Z.-G. Rong, Optimization of flocculation conditions for kaolin suspension using the composite flocculant of MBFGA1 and PAC by response surface methodology, Bioresour. Technol. 100 (2009) 4233–4239.
[24] N. Zaghbani, A. Hafiane, M. Dhahbi, Separation of methylene blue from aqueous solution by micellar enhanced ultrafiltration, Sep. Purif. Technol. 55 (2007) 117–124.
[25] M. Sarkar, S. Poddar, Studies on the interaction of surfactants with cationic dye by absorption spectroscopy, J. Colloid Interface Sci. 221 (2000) 181–185.
[26] Z. Zhao, Micellar Catalysis and Microemulsion Catalysis, Chem. Indust. Press, Beijing, 2006.
[27] E. Rodenas-Torralba, B.F. Reis, A. Morales-Rubio, M. de la Guardia, An environmentally friendly multicommutated alternative to the reference

method for anionic surfactant determination in water, Talanta 66 (2005) 591–599.
[28] D. Miller, Binding of calcium ions to micelles—a metallochromic indicator study, Colloid Polym. Sci. 267 (1989) 929–934.
[29] A. Zapf, R. Beck, G. Platz, H. Hoffmann, Calcium surfactants: a review, Adv. Colloid Interface Sci. 100 (2003) 349–380.
[30] P.K. Sen, S. Talukder, B. Pal, Specific interactions of anions and pre-micelles in the alkaline fading of crystal violet carbocation, Colloids Surf. A 467 (2015) 259–269.
[31] S.L. Young, E. Matijević, Precipitation phenomena of heavy metal soaps in aqueous solutions: III. Metal laurates, J. Colloid Interface Sci. 61 (1977) 287–301.
[32] Y. Huang, G. Han, J. Liu, W. Wang, A facile disposal of Bayer red mud based on selective flocculation desliming with organic humics, J. Hazard. Mater. 301 (2016) 46–55.
[33] Y.Y. Zhang, Z.H. Yang, G.M. Zeng, J. Huang, S.M. Wei, J. Feng, Microbial flocculant MBFGA1 preliminary structure identification and research on flocculation mechanism, Environ. Sci. 33 (2013) 278–285 (in Chinese).
[34] B.J. Lee, M.A. Schlautman, E. Toorman, M. Fettweis, Competition between kaolinite flocculation and stabilization in divalent cation solutions dosed with anionic polyacrylamides, Water Res. 46 (2012) 5696–5706.